Research Article | Vol. 27, No. 10 | 13 May 2019 | OPTICS EXPRESS 13820
Optics EXPRESS

Heterodyne interferometer with two parallel-polarized input beams for high-resolution roll angle measurement

JINGYA QI,[1] ZHAO WANG,[1,*] JUNHUI HUANG[1], QING WANG[2] AND JIANMIN GAO[3]

[1]School of Mechanical Engineering, Xi'an Jiaotong University, Xi'an, 710049, China
[2]Department of Engineering, Durham University, Durham, DH13LE, UK
[3]Western China Institute of Quality Science and Technology, Xi'an Jiaotong University, Xi'an, 710049, China
*wangzhao@mail.xjut.edu.cn

Abstract: We have proposed an improved heterodyne interferometric roll measurement system with enhanced resolution in this paper. Two beams with different frequencies but with the same polarization state input to the interferometer are provided by two acousto-optic modulators. A quarter-wave plate is employed in each path before the two beams are combined to generate a beat frequency. A mathematical model for the measurement system is established based on Jones' calculus. The measurement resolution is doubled because the sensitive areas of the two beams appear simultaneously. Experimental results show that in the range of 0.1° the gain coefficient reaches 229 which is twice that of the traditional method.

1. Introduction

Translation guideway is the key part of industrial precision equipment such as the numerically controlled machine tools, lithography machines and coordinate measuring machines. Accurate measurement of the roll angle of the translation stage is directly subject to the property and specification of the equipment. The roll angle is required to be measured to improve the manufacturing process or measuring precision.

The heterodyne interferometer has emerged as a promising route for geometric error measurement for its high resolution, high precision, and less sensitive to the environment. Many research based on this instrument has been carried out for the measurement of displacement [1–5], straightness error [6–8], pitch and yaw errors [9–13]. However, the roll angle, as an in-plain error, does not bring any optical path length (OPL) change in a standard Michelson interferometer. Some improvements are reported to solve this problem. A wedge prism and a wedge mirror are set in the interferometer so that the roll displacement of the wedge prime will induce an OPL change in the measuring arm [14,15]. This method detects the phase shift that is caused by the change of OPL. On the other hand, a method of detecting the phase shift caused by the change of the polarization state is also very popular. B.P. Cornonkevich firstly came up with a structure which used a polarizer as the measuring plate [16]. In his work, a dual-frequency light from a Zeeman laser with two polarization-orthogonal frequencies (f_1 and f_2) was used as the measuring source. After passing the polarizer, the beam with a beat frequency of f_1-f_2 was generated and received by a photodetector as the measurement signal. The phase of the measurement signal has a synchronous fluctuation with the roll of the polarizer. Combined with a reference signal, the phase shift can be detected to calculate the roll error. Hong Jiang et al. proposed a method adding a quarter wave plate (QWP) right after the emitted source [16,17]. The fast axis of QWP was set a small deviation angle of θ from the polarization state of the TM beam, which dramatically improved the measurement resolution. The roll angle of the polarizer is

#361944 https://doi.org/10.1364/OE.27.013820
Journal © 2019 Received 11 Mar 2019; revised 20 Apr 2019; accepted 21 Apr 2019; published 29 Apr 2019

converted into an observable phase shift of the measurement beam, so the roll error is derived by detecting the phase change.

It is known that when a half wave plate (HWP) is rotated by $\alpha°$, the polarization of the light passing through it is rotated by $2\alpha°$ in the same direction. We can deduce that if a HWP is used as the sensor-plate before the polarizer, the measurement resolution can be doubled. Liu et al. proposed a method of the beam passing back and forth through the HWP, which increased the measurement resolution again [18]. The result of a beam passing back and forth through a HWP is equivalent to the superimposition of two single-passes. Tang et al. then achieved a scheme of multi-passing the HWP, so the sensitivity was greatly increased [19,20]. In our previous work [22], we proposed a differential heterodyne interferometric configuration, which employs the previously unchanged reference beam as another measurement beam. Owing to the opposite phase shift of this second measurement signal, the measurement sensitivity can be doubled.

The phase shift, as the output of the interferometer, is composed of the phase shifts of two beams with different frequencies. All of the sources used in previous heterodyne roll measurement interferometers were orthogonally polarized dual-frequency lasers provided by Zeeman split or modulated acousto-optic modulators (AOM) [16–22]. The phase shift of each mode shows a high sensitivity within a specific roll area, called the sensitive area, in which the roll error is converted to a detectable phase shift by the gain factor. However, the sensitive areas of the two modes do not appear simultaneously because the polarization states of the two beams with different frequencies are perpendicular to each other. Since the beat signal is generated by these two modes, the final readout only has the gain coefficient of one beam instead of the superposition of two beams.

For this concern, we propose another improved interferometric heterodyne method for the roll measurement. It also achieves a twice resolution as the same as the differential interferometer. The difference is that the gain factor of the only measurement beam is amplified in this method. In this configuration, two AOMs are used to generate two modes with different frequencies but with the same polarization state. After respectively passing through two QWPs which are carefully oriented at different angles, the two beams are merged into a dual-frequency light. A HWP is utilized as the measuring sensor. The sensitive areas of the two single-frequency beams overlap in this structure. As a result, the gain coefficient of the heterodyne signal in the sensitive area is significantly enhanced. The roll angle is determined by the gain coefficient of the heterodyne signal, so the measurement resolution is doubled in comparison to that of the standard configuration.

2. Measurement principle

2.1 Previous roll interferometer with orthogonally polarized laser source

To understand the drawback of the previous interferometers, the principles of the two structures are introduced here. For the scheme of single-pass in [17], the polarization states of the measurement light passing the optical plates are explained in detail as follows. The laser source contains two orthogonally polarized beams with frequency f_1 and f_2. Two beams with frequency f_1 and f_2 are coaxial but they are displayed separately for clarity in Fig. 1.

As shown in Fig. 1(a), for the beam f_1, the linearly polarized laser Ei_{f1} is turned into an elliptically polarized beam after passing the QWP. The elliptically polarized beam is equivalent to two coaxial linearly polarized lights Ef_{f1} and Es_{f1} whose polarization states are along the fast and slow axes of the QWP, respectively, and with a phase difference of 90°. The two linearly polarized lights can be written as

$$Ef_{f_1} = Ei_{f_1} \cos\theta. \tag{1}$$

$$Es_{f_1} = Ei_{f_1} \sin\theta \exp(\pi/2). \tag{2}$$

where $Ei_{f1} = E\cos(\omega_1 t + \varphi_1)$.

Then these two beams interfere with each other on the transmission axis of the polarizer (P). The phase of interfered beam Eo_{f1} is related to $E1_{f1}$ and $E2_{f1}$, which are the projection of Ef_{f1} and Es_{f1} on the transmission axis as shown in Fig. 1(b). Two projections $E1_{f1}$ and $E2_{f1}$ are given by

$$E1_{f_1} = Ei_{f_1}\cos\theta\cos\gamma = E\cos\theta\cos\gamma\cos(\omega_1 t + \varphi_1). \tag{3}$$

$$E2_{f_1} = Ei_{f_1}\sin\theta\sin\gamma\exp(\pi/2) = E\sin\theta\sin\gamma\cos(\omega_1 t + \varphi_1 + \pi/2). \tag{4}$$

Setting $A_1 = E\cos\theta\cos\gamma$, $A_2 = E\sin\theta\sin\gamma$, the interfered beam Eo_{f1} is calculated as

$$\begin{aligned} Eo_{f_1} &= A_1\cos(\omega_1 t + \varphi_1) + A_2\cos(\omega_1 t + \varphi_1 + \pi/2) \\ &= A_{f_1}\cos(\omega_1 t + \varphi_1 + \psi_{f_1}). \end{aligned} \tag{5}$$

where $A_{f_1} = \sqrt{A_1^2 + A_2^2}$ and the phase shift is given by

$$\psi_{f_1} = \tan^{-1}(A_2/A_1) = \tan^{-1}(\tan\theta\cdot\tan\gamma). \tag{6}$$

The derivative of the phase shift is then given by

$$K_{f_1} = \mathrm{d}\psi_{f_1}/\mathrm{d}\gamma = \frac{1}{\cos^2\gamma + \tan^2\theta\sin^2\gamma}. \tag{7}$$

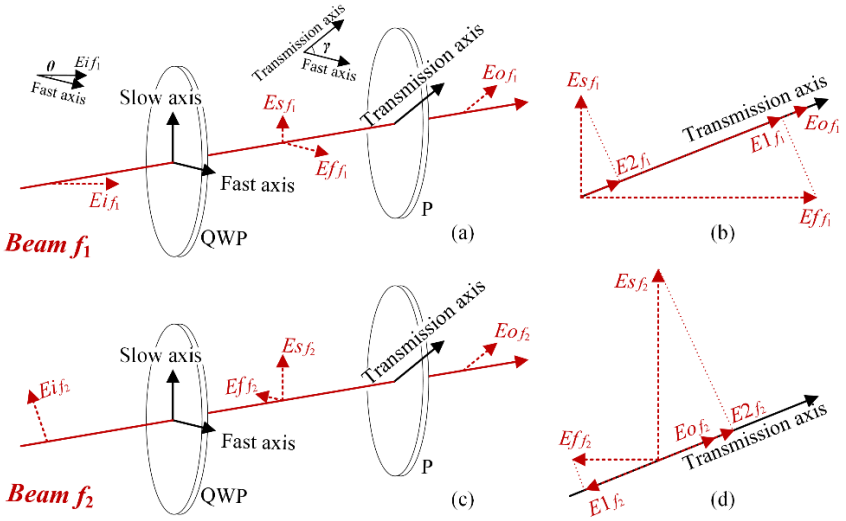

Fig. 1. The polarization states of the beam passing through QWP and polarizer.

The small roll of γ is magnified into a detectable phase shift by K_{f1} times. Note that the orientation of QWP θ is quite small. It can be seen from Eq. (7) that when $\gamma = 90°$, K_{f1} is maximum. This means that when the transmission axis of the polarizer approaches the slow axis of QWP, the phase-shift change of the measuring beam Eo_{f1} caused by the roll angle is large. Obviously, high measurement resolution requires large roll-induced phase change, so the high-resolution roll is supposed to be measured in this particular region, named the sensitive area. It also can be seen from Eq. (7) that the smaller θ is, the higher K_{f1} is in the sensitive area. That explains why θ was set as a small orientation in the measurement. However, it comes at the cost of severe intensity drop [17]. Therefore, the angle of the QWP θ cannot be too small.

In the same way, the polarization state change of the beam Ei_{f2} is shown in Figs. 1(c) and (d). The phase shift of the output beam Eo_{f2} is given by

$$\psi_{f_2} = \tan^{-1}(\cot\theta \cdot \tan\gamma). \tag{8}$$

Its derivative is calculated as

$$K_{f_2} = \mathrm{d}\psi_{f_2}/\mathrm{d}\gamma = \frac{1}{\cos^2\gamma + \cot^2\theta \sin^2\gamma}. \tag{9}$$

Two output beams Eo_{f1} and Eo_{f2} eventually generate a beat signal as follows:

$$Eo = E\cos\left[(\omega_1 - \omega_2)t + (\varphi_1 - \varphi_2) + (\psi_{f_1} - \psi_{f_2})\right]. \tag{10}$$

The phase shift of the measured signal is composed of the shifts of two parts. However, it can be seen from Eqs. (7) and (9) that the change of the phase shift of beam f_1 is maximum when $\gamma = 90°$, while the maximum phase change for beam f_2 locates at $\gamma = 0°$. The sensitive areas of beams f_1 and f_2 are shifted by 90° so that the sensitive area of the final heterodyne signal appears every 90°, and the gain coefficient is the same as that of one single-frequency beam.

A more complicated one-bounce scheme that has higher measurement resolution is present in Fig. 2 [18]. The reference beam is unchanged so that it is not shown here. A HWP is used as the sensor-plate and the measurement beam passes through the HWP twice. When the HWP is rotated by $\alpha°$, the polarization of the returning beam has a rotation of $4\alpha°$. Therefore, the phase shift of the heterodyne signal would have a sensitive area every 22.5°. The phase difference between the reference and measurement signals is given by

$$\psi = \psi 1 - \psi 2 = -\tan^{-1}(\tan\theta \tan 4\alpha) - \left[-\tan^{-1}(\cot\theta \tan 4\alpha)\right]. \tag{11}$$

where $\psi 1$ and $\psi 2$ are the phase shifts of beams f_1 and f_2, respectively.

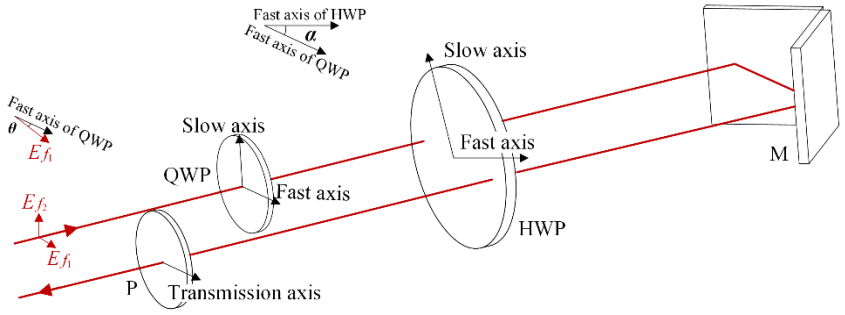

Fig. 2. Schematic of measurement arm of the previous roll interferometer.

Figure 3 shows the theoretical unwrapped phase shift versus the roll angle of the HWP. The phase shift of the measurement signal in Fig. 3(a) is the phase shift of beam f_1 minus that of beam f_2. The phase shifts of beams f_1 and f_2 are shown in Fig. 3(b). The region where the phase shift change is sharp is the sensitive area. It is clear that the sensitive area of beam f_1 (e.g. Point A) corresponds to the non-sensitive area of beam f_2 (e.g. Point B). Similarly, the sensitive area of beam f_2 (e.g. Point C) corresponds to the non-sensitive area of beam f_1 (e.g. Point D). As analyzed above, the sensitive areas of two beams appear alternately and have a roll distance of 22.5°. This is because the source beams f_1 and f_2 are mutually perpendicular. As a result, the sensitive areas of the composed heterodyne signal show up at the sensitive areas of both beam f_1 and beam f_2, but the gain coefficient of the heterodyne signal is only equal to that of one of the beams. Another beam hardly contributes to the gain coefficient value.

Optics EXPRESS

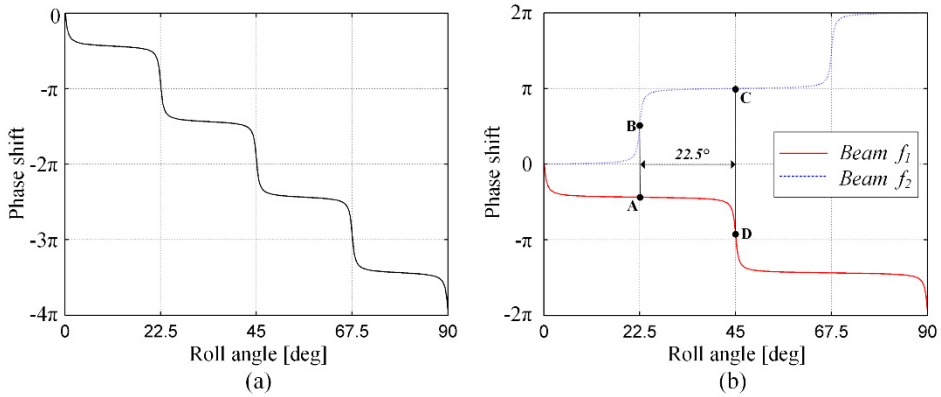

Fig. 3. Calculated phase shifts versus roll angle for the traditional method. (a) Phase shift of the heterodyne signal. (b) Phase shifts of two single-frequency beams.

2.2 Resolution-enhanced heterodyne roll measurement interferometer

An improved roll measurement system with an enhanced resolution is shown in Fig. 4. The beam from a stabilized single-frequency He-Ne laser is equally split by a beam splitter (BS1) into two beams. Then the two beams are directed in two AOMS (AOM1 and AOM2 respectively) which are driven by two different radio frequency (RF) signals using separate RF drivers. Two diffracted beams are modulated into two different frequency shifts, respectively. The AOM is commonly used to frequency-shift light by Bragg diffraction. The angle of incidence light into the AOM should be set as the Bragg angle so that most intensity is distributed to the first diffraction order light. Note that the beams off two AOMs have the same polarization state, which is the key part of this construction.

The two diffraction beams proceed to the quarter-wave plates (QWP1 and QWP2) in the respective propagation paths and recombine on BS2. One of the beams exiting BS2 is directly received by a polarizer (P1) and a photodetector (PD1) and becomes the reference signal. The frequency of the reference signal is f_1-f_2. The other dual-frequency beam generated by BS2 is used as the measurement beam. The measurement beam transmits through the sensor HWP and is then reflected back off a folding mirror made by two mirrors forming a right-angle dihedral. The beam then passes the HWP again and is collected by another photodetector (PD2) preceded by a polarizer (P2). The measurement signal has the same f_1-f_2 frequency as the reference but it is phase shifted in accordance with the roll information.

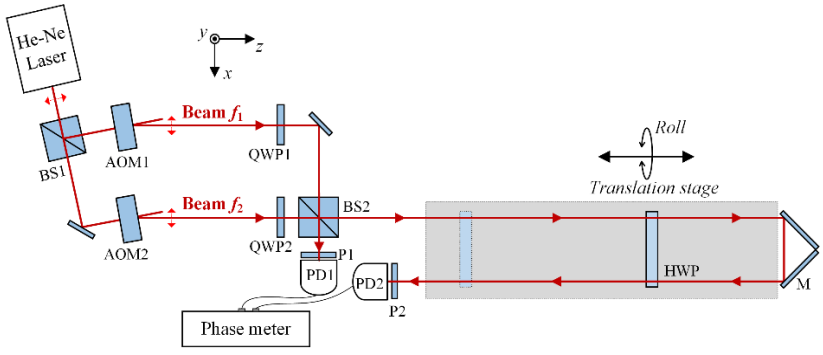

Fig. 4. Schematic of the improved heterodyne interferometer for the roll angle measurement.

As shown in Fig. 4, the z axis is along the translation direction and the x axis is set to parallel to the polarization state of the input measurement beam. The QWPs are oriented at

Optics EXPRESS

angles θ_1 and θ_2, and θ_2-θ_1 = π/2. The Jones' matrix calculation enables us to calculate the phase shift of measurement single by following the scheme in Fig. 4.

The Jones' vectors of the polarization states of the two input beams diffracted by the AOMS are written as

$$B_1 = \begin{bmatrix} E\exp\left[i(\omega_1 t+\varphi_1)\right] \\ 0 \end{bmatrix}, B_2 = \begin{bmatrix} E\exp\left[i(\omega_2 t+\varphi_2)\right] \\ 0 \end{bmatrix}.$$

QWP1 and QWP2, HWP and P are written as

$$Q_1 = \begin{bmatrix} \cos^2\theta_1 + i\sin^2\theta_1 & (1-i)\sin\theta_1\cos\theta_1 \\ (1-i)\sin\theta_1\cos\theta_1 & \sin^2\theta_1 + i\cos^2\theta_1 \end{bmatrix}, Q_2 = \begin{bmatrix} \cos^2\theta_2 + i\sin^2\theta_2 & (1-i)\sin\theta_2\cos\theta_2 \\ (1-i)\sin\theta_2\cos\theta_2 & \sin^2\theta_2 + i\cos^2\theta_2 \end{bmatrix},$$

$$H(\alpha) = \begin{bmatrix} \cos 2\alpha & \sin 2\alpha \\ \sin 2\alpha & -\cos 2\alpha \end{bmatrix}, P = \begin{bmatrix} 1 & 0 \end{bmatrix}.$$

The measurement light E_m is expressed as

$$E_m = PH(-\alpha)H(\alpha)\left(Q_1B_1 + Q_2B_2\right). \tag{12}$$

Substituting the above values into Eq. (12), we can obtain

$$E_m = E_1\exp\left(\omega_1 t+\varphi_1+\psi_1\right) + E_2\exp\left(\omega_2 t+\varphi_2+\psi_2\right). \tag{13}$$

where E_1 and E_2 are the amplitudes of Beams f_1 and f_2. ψ_1 and ψ_2 are the phase shifts of Beams f_1 and f_2. They are given by

$$E_1 = E\sqrt{\left[\cos\theta_1\cos\left(4\alpha-\theta_1\right)\right]^2 + \left[\sin\theta_1\sin\left(4\alpha-\theta_1\right)\right]^2}. \tag{14}$$

$$E_2 = E\sqrt{\left[\cos\theta_2\cos\left(4\alpha-\theta_2\right)\right]^2 + \left[\sin\theta_2\sin\left(4\alpha-\theta_2\right)\right]^2}. \tag{15}$$

$$\psi_1 = \tan^{-1}\left[\tan\theta_1\tan\left(4\alpha\right)\right]. \tag{16}$$

$$\psi_2 = \tan^{-1}\left[\tan\theta_2\tan\left(4\alpha\right)\right]. \tag{17}$$

The irradiance of the light produced in PD2 is $I = E_m^2$, so the intensity of the measurement light is expressed as

$$I = E^2 + E_1E_2\left[\cos\left(\omega_1-\omega_2\right)t + \left(\varphi_1-\varphi_2\right) + \psi_1 - \psi_2\right]. \tag{18}$$

After decoupling the DC term by a high pass filter, the measurement signal is written as

$$D_m = \mathrm{A}\left[\cos\left(\omega_1-\omega_2\right)t + \left(\varphi_1-\varphi_2\right) + \psi_1 - \psi_2\right]. \tag{19}$$

where A combines factors of AC light power E_1E_2 and the photodiode efficient. Since the phase of the reference is nominally constant, the phase difference between two signals can be expressed as

$$\begin{aligned} \psi(\alpha) &= \psi_1 - \psi_2 \\ &= -\tan^{-1}\left[\tan\theta_1\tan\left(4\alpha\right)\right] - \left\{-\tan^{-1}\left[\tan\theta_2\tan\left(4\alpha\right)\right]\right\} \\ &= -2\tan^{-1}\left[\tan\theta_1\tan\left(4\alpha\right)\right]. \end{aligned} \tag{20}$$

Optics EXPRESS

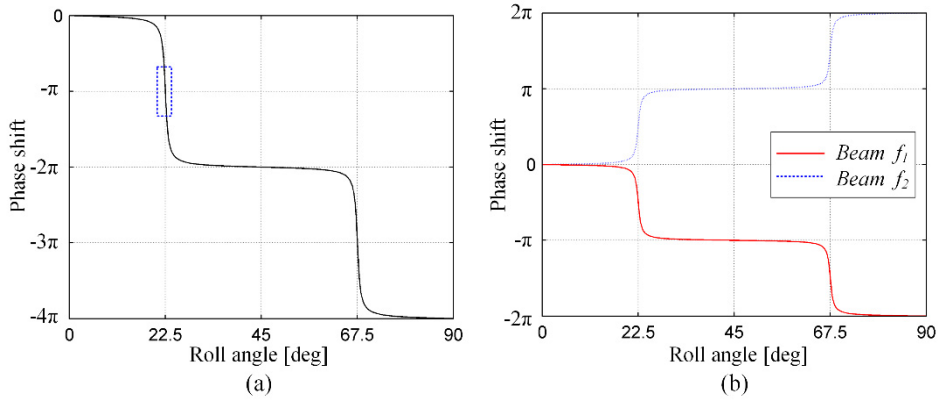

Fig. 5. The theoretical unwrapped phase shifts versus roll angle for the proposed method. (a) Phase shift of the heterodyne signal. (b) Phase shifts of two single-frequency beams.

Figure 5 illustrates the phase shift of the measurement signal of the proposed configuration when $\theta_1 = 2°$ and $\theta_2 = 92°$. The phase shift of the beat signal, which contains those of the two single-frequency beams, is shown in Fig. 5(a). The phase shifts of beams f_1 and f_2 caused by the roll angle show opposite shift directions, as seen in Fig. 5(b), and the two curves have their sensitive areas at the same roll value. So, the gain coefficient of the heterodyne signal is significantly enhanced. The roll-induced phase shift is quasi-linear in a small area in the blue dotted diagram in Fig. 5(a). The calculated roll can be derived from

$$\Delta\alpha = \Delta\psi / G. \tag{21}$$

where G is the gain coefficient in the sensitive area. In this way, the small roll error is amplified into an observable phase change. A measuring error caused by the fitting error is about 0.2 arcsec in a measurement range of 0.1°. Providing that $\tan\Delta\alpha \approx k\Delta\alpha$, we can obtain G from Eq. (20) as

$$G = 8\cot\theta_1. \tag{22}$$

Compared with the traditional method, the gain coefficient is doubled for the improved configuration. We can also draw this conclusion by comparing the sensitive areas in Figs. 3(a) and 5(a). Consequently, the measurement resolution for roll error is enlarged twofold employing a phase-meter with same level resolution.

3. Experiment and results

To evaluate the proposed roll measurement interferometric method, an experimental setup was built, as shown in Fig. 6. A single-frequency He-Ne laser (05STP910, Melles Griot Co., USA) was employed as the source. The laser was then split into two by BS1. Two beams were launched into two AOMs (3080-125, Gooch & Housego Co., UK) that were driven by two RF drivers (AODS Synth DDS 8 CH, Gooch & Housego Co., UK), respectively. The AOM adds a specific frequency shift to each beam which is dependent on the RF drive signal into the AOM crystal. The incidence of light into the AOM should be carefully controlled at the Bragg Angle to distribute light intensity into the first diffraction order. In this experiment, two RF signals were set as 80 MHz and 80.05 MHz, respectively. The orientations of QWP1 and QWP2 were set as $\theta_1 = 2$ and $\theta_2 = 92$. The heterodyne frequency detected by the reference and measurement photodetectors PD1 and PD2 (PAP36A, Thorlabs Co., USA) was 50kHz consequently. The phase difference between PD1 and PD2 was read by an FFT phase meter (6000A, Clarke-Hess Co., USA).

Optics EXPRESS

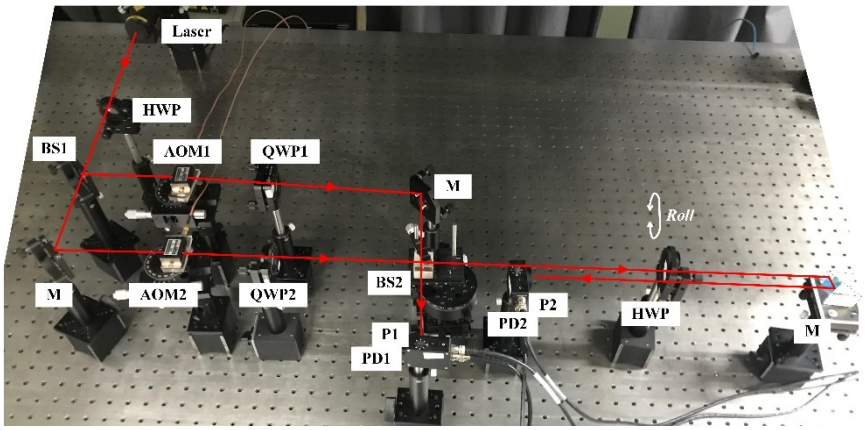

Fig. 6. Experimental setup for the interferometric roll measurement.

The experimental result of phase difference versus the roll angle is shown in Fig. 7. In the roll range of 90°, reasonable agreement is seen between calculated and experimental results. It is pretty clear that the sensitive area of the proposed interferometer is located between Points A and B in Fig. 7.

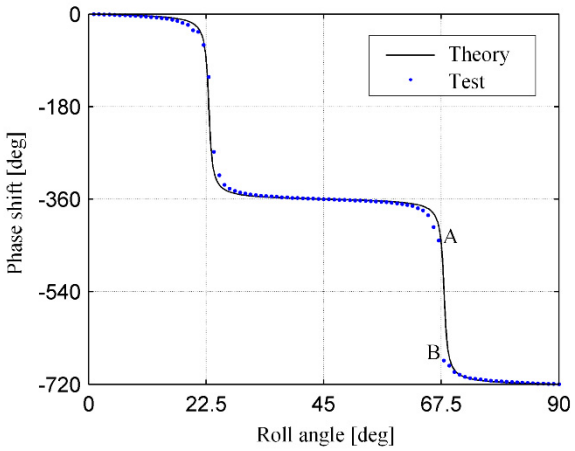

Fig. 7. Experimental results of the improved interferometer and its theoretical curve in the range of 90°.

To calibrate the gain coefficient, a tilt stage resolving 0.01° was utilized to perform the specific roll angles, and a commercial interferometer (XL-80, Renishaw Co., UK) was utilized to measure the roll at the same time as the benchmark as shown in Fig. 8. The movement of the tilt table is a roll motion to our system but a tilt motion to the Renishaw calibrator. The HWP was rotated into a middle point between Points A and B in Fig. 7. Then the tilt stage was rotated at a step of 0.01° along the roll direction for 3 trials. The variation of average phase shifts of 3 tests is quasi-linear within 0.1° as displayed in Fig. 9(a). The average and fitted curves are shown in Fig. 9(b). Fitted by the least-square method, the gain coefficient of the line turns out to be $G = 229$. The experimental gain coefficient is the same as the theoretical value calculated in Eq. (22) showing that the proposed improved interferometer acquires enhanced measurement resolution. The residuals between the roll measured by the calculated G and that measured by Renishaw calibrator are also shown in Fig. 9(b). The maximum residual is about 8 arcsec with a standard deviation of 4.5 arcsec, which may be caused by the drift of the measured phase and the vibration of the HWP.

Optics EXPRESS

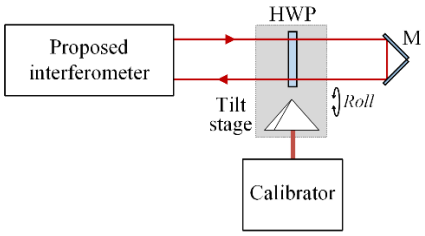

Fig. 8. Schematic setup of the improved interferometer and the commercial calibrator.

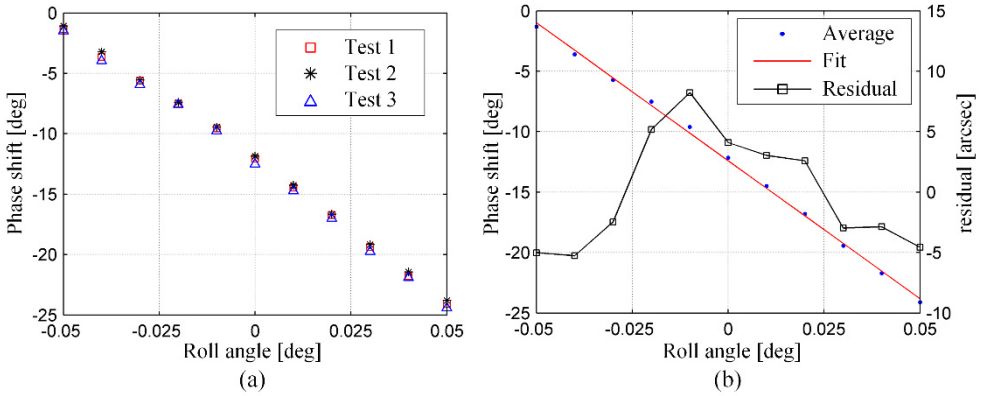

Fig. 9. Experimental result of phase shifts versus roll angle in the sensitive area. (a) Experimental results of 3 trials. (b) Average data, fitted line and residual.

A drift test was conducted by monitoring the interferometer beat frequency and phase shift readouts while the sensor plate remained stationary to evaluate the stability of the system. Figure 10 (a) shows that the frequency of the heterodyne signal is about 49.955 kHz with a standard deviation of 5Hz. It is seen from Fig. 10(b) that the fluctuation of the measured phase shift was almost in a limitation of 0.03°. We attribute this to the laser drift, air turbulence, instability of the phase meter, and the statistic limits which include the quantum noise (shot noise) and the detector noise. Since the severely attenuated intensity of the AC signal, the detector noise limits our results over the shot noise [17,23]. An ideal measurement resolution about 0.03/G = 0.47 arcsec is expected to be attained considering all the above factors. The environmental factor can be reduced by using polarization maintaining optical fibers to direct the beams into the interferometer [3]. Thus, the exothermic laser source is kept away from the optical structure, which can strengthen the resistance to the fluctuation of the refractive index of air.

Finally, a test for the roll of a tilt stage was carried out. In this test, the tilt stage was automatically driven at a step of 0.01°. The data process collected one data point every 0.5 second from the phase meter. For each roll angle, one set of data (approximately 30 sampling points) was recorded. The roll motion was measured by the Renishaw calibrator at the same time. Figure 11 displays the test results showing that our system has good performance for the roll measurement. The maximum residual is 7.8 arcsec compared with the results of the calibrator. At the same time, the average value of one set of measured data for one roll position is compared with that of the calibrator results. The maximum average value difference is about 2.8 arcsec.

Optics EXPRESS

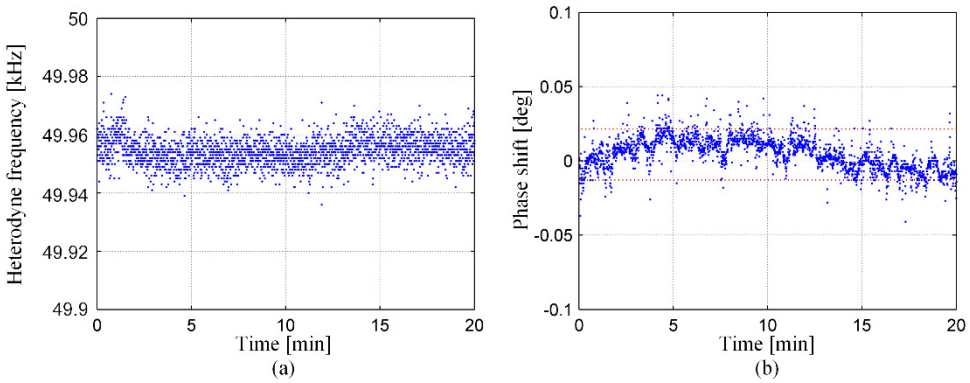

Fig. 10. Stability of the readout of interferometer. (a) Heterodyne frequency stability. (b) Phase shift stability.

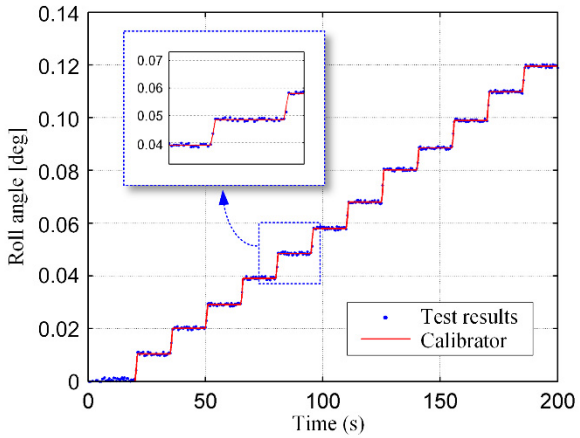

Fig. 11. Experimental results for roll angle test of the tilt table.

We have demonstrated the differential interferometer in [22], which employed the reference beam as another measurement beam entering the measurement arm to achieve a double measurement resolution. To step forward, we could apply this idea in the scheme proposed in this manuscript. Thus, determined by the phase difference of two updated measurement signals, the measurement resolution is expected to be enhanced by about four times. Extended analysis and experimental verification of this next generation interferometer are the future work for high-precision roll measurement.

4. Conclusion

In summary, we have proposed and verified an improved heterodyne interferometer for the roll angle measurement. The measurement system generates two modes with different frequencies but the same polarization state by using two AOMs. The sensitive areas of two beams appear at the same time so that the phase shift of the beat signal has a dramatically enhanced gain coefficient in its sensitive area. Thus, the measurement resolution is enhanced twofold in comparison with the traditional interferometer. The experimental setup was conducted to verify the performance of the new configuration. An experimental gain coefficient of 229 was obtained. Taking the air turbulence, statistic noise and other effects into consideration, a theoretical measurement resolution about 0.47 arcsec was confirmed.

Optics EXPRESS

The feasibility was validated by the roll displacement measurement of a precision tilt stage with a measurement accuracy of 7.8 arcsec.

Funding

National Natural Science Foundation of China (NSFC) (61405156); China Sponsorship Council (CSC) (201806280163).

References

1. N. Bobroff, "Recent advances in displacement measuring interferometry," Meas. Sci. Technol. **4**(9), 907–926 (1993).
2. K. N. Joo, J. D. Ellis, E. S. Buice, J. W. Spronck, and R. H. M. Schmidt, "High resolution heterodyne interferometer without detectable periodic nonlinearity," Opt. Express **18**(2), 1159–1165 (2010).
3. S. Zhao, H. Wei, M. Zhu, and Y. Li, "Green laser interferometric metrology system with sub-nanometer periodic nonlinearity," Appl. Opt. **55**(11), 3006–3011 (2016).
4. E. Zhang, B. Chen, H. Zheng, L. Yan, and X. Teng, "Laser heterodyne interferometer with rotational error compensation for precision displacement measurement," Opt. Express **26**(1), 90–98 (2018).
5. X. Xing, D. Chang, P. Hu, and J. Tan, "Spatially separated heterodyne grating interferometer for eliminating periodic nonlinear errors," Opt. Express **25**(25), 31384–31393 (2017).
6. T. Jin, H. Ji, W. Hou, Y. Le, and L. Shen, "Measurement of straightness without Abbe error using an enhanced differential plane mirror interferometer," Appl. Opt. **56**(3), 607–610 (2017).
7. B. Chen, L. Cheng, L. Yan, E. Zhang, and Y. Lou, "A heterodyne straightness and displacement measuring interferometer with laser beam drift compensation for long-travel linear stage metrology," Rev. Sci. Instrum. **88**(3), 035114 (2017).
8. Q. Chen, D. Lin, J. Wu, J. Yan, and C. Yin, "Straightness/coaxiality measurement system with transverse Zeeman dual-frequency laser," Meas. Sci. Technol. **16**(10), 2030–2037 (2005).
9. H. Schwenke, W. Knapp, H. Haitjema, A. Weckenmann, R. Schmitt, and F. Delbressine, "Geometric error measurement and compensation of machines—An update," CIRP Annals - Manufacturing Technology **57**(2), 660–675 (2008).
10. S. R. Gillmer, R. C. G. Smith, S. C. Woody, and J. D. Ellis, "Compact fiber-coupled three degree-of-freedom displacement interferometry for nanopositioning stage calibration," Meas. Sci. Technol. **25**(7), 075205 (2014).
11. E. Zhang, Q. Hao, B. Chen, L. Yan, and Y. Liu, "Laser heterodyne interferometer for simultaneous measuring displacement and angle based on the Faraday effect," Opt. Express **22**(21), 25587–25598 (2014).
12. H. Yan, H. Z. Duan, L. T. Li, Y. R. Liang, J. Luo, and H. C. Yeh, "A dual-heterodyne laser interferometer for simultaneous measurement of linear and angular displacements," Rev. Sci. Instrum. **86**(12), 123102 (2015).
13. X. Yu, S. R. Gillmer, S. C. Woody, and J. D. Ellis, "Development of a compact, fiber-coupled, six degree-of-freedom measurement system for precision linear stage metrology," Rev. Sci. Instrum. **87**(6), 065109 (2016).
14. T. Jin, G. Xia, W. Hou, Y. Le, and S. Han, "High resolution and stability roll angle measurement method for precision linear displacement stages," Rev. Sci. Instrum. **88**(2), 023102 (2017).
15. K. Shi, J. Su, and W. Hou, "Roll angle measurement system based on differential plane mirror interferometer," Opt. Express **26**(16), 19826–19834 (2018).
16. H. Jiang and C. Yin, "Sensitivity enhanced roll angle measurement," Opt. Eng. **39**(2), 516–519 (2000).
17. S. R. Gillmer, J. Martínez-Rincón, and J. D. Ellis, "Anomalous vibration suppression in a weak-value-emulated heterodyne roll interferometer," Opt. Express **26**(22), 29311–29318 (2018).
18. Z. Liu, D. Lin, H. Jiang, and C. Yin, "Roll angle interferometer by means of wave plates," Sens. Actuators A Phys. **104**(2), 127–131 (2003).
19. S. Tang, Z. Wang, M. Li, W. Zhang, F. Yang, and X. Zhang, "Note: A small roll angle measurement method with enhanced resolution based on a heterodyne interferometer," Rev. Sci. Instrum. **86**(9), 096104 (2015).
20. S. Tang, Z. Wang, M. Li, J. Gao, Y. Jiang, and Y. Zhang, "Note: Optimal choice of the reflector by phase analysis for heterodyne interferometric roll angle measurement," Rev. Sci. Instrum. **87**(2), 026101 (2016).
21. C. M. Wu and Y. T. Chuang, "Roll angular displacement measurement system with microradian accuracy," Sens. Actuators A Phys. **116**(1), 145–149 (2004).
22. J. Qi, Z. Wang, J. Huang, and J. Gao, "Resolution-enhanced heterodyne laser interferometer with differential configuration for roll angle measurement," Opt. Express **26**(8), 9634–9644 (2018).
23. J. Lawall and E. Kessler, "Michelson interferometry with 10 pm accuracy," Rev. Sci. Instrum. **71**(7), 2669-2676 (2000).